

Assessing the distinguishable cluster approximation based on the triple bond-breaking in the nitrogen molecule

Varun Rishi, Ajith Perera, and Rodney J. Bartlett

Citation: *J. Chem. Phys.* **144**, 124117 (2016); doi: 10.1063/1.4944087

View online: <http://dx.doi.org/10.1063/1.4944087>

View Table of Contents: <http://aip.scitation.org/toc/jcp/144/12>

Published by the [American Institute of Physics](#)

Assessing the distinguishable cluster approximation based on the triple bond-breaking in the nitrogen molecule

Varun Rishi, Ajith Perera, and Rodney J. Bartlett^{a)}

Quantum Theory Project, University Of Florida, Gainesville, Florida 32611, USA

(Received 13 November 2015; accepted 2 March 2016; published online 31 March 2016)

Obtaining the correct potential energy curves for the dissociation of multiple bonds is a challenging problem for *ab initio* methods which are affected by the choice of a spin-restricted reference function. Coupled cluster (CC) methods such as CCSD (coupled cluster singles and doubles model) and CCSD(T) (CCSD + perturbative triples) correctly predict the geometry and properties at equilibrium but the process of bond dissociation, particularly when more than one bond is simultaneously broken, is much more complicated. New modifications of CC theory suggest that the deleterious role of the reference function can be diminished, provided a particular subset of terms is retained in the CC equations. The Distinguishable Cluster (DC) approach of Kats and Manby [J. Chem. Phys. **139**, 021102 (2013)], seemingly overcomes the deficiencies for some bond-dissociation problems and might be of use in quasi-degenerate situations in general. DC along with other approximate coupled cluster methods such as ACCD (approximate coupled cluster doubles), ACP-D45, ACP-D14, 2CC, and pCCSD(α , β) (all defined in text) falls under a category of methods that are basically obtained by the deletion of some quadratic terms in the double excitation amplitude equation for CCD/CCSD (coupled cluster doubles model/coupled cluster singles and doubles model). Here these approximate methods, particularly those based on the DC approach, are studied in detail for the nitrogen molecule bond-breaking. The N_2 problem is further addressed with conventional single reference methods but based on spatial symmetry-broken restricted Hartree–Fock (HF) solutions to assess the use of these references for correlated calculations in the situation where CC methods using fully symmetry adapted SCF solutions fail. The distinguishable cluster method is generalized: 1) to different orbitals for different spins (unrestricted HF based DCD and DCSD), 2) by adding triples correction perturbatively (DCSD(T)) and iteratively (DCSDT-n), and 3) via an excited state approximation through the equation of motion (EOM) approach (EOM-DCD, EOM-DCSD). The EOM-CC method is used to identify lower-energy CC solutions to overcome singularities in the CC potential energy curves. It is also shown that UHF based CC and DC methods behave very similarly in bond-breaking of N_2 , and that using spatially broken but spin preserving SCF references makes the CCSD solutions better than those for DCSD. © 2016 AIP Publishing LLC. [<http://dx.doi.org/10.1063/1.4944087>]

I. INTRODUCTION

Coupled Cluster¹ (CC) theory is the method of choice for providing molecular properties at equilibrium geometry. But as we stretch the bonds, the underlying assumption of a single reference (SR) approximation (Hartree-Fock (HF) or other), particularly in its spin restricted form, fails to describe the system and consequently, correlation methods such as CC built on this approximation fail as well.² While spin-symmetry broken solutions such as unrestricted HF (UHF) fix some, but not all of these problems, they also raise new issues such as spin contamination. The prototype for such bond-breaking studies is offered by the N_2 molecule as has been apparent from CC's inception.^{2–5} Coupled cluster methods based on a restricted HF (RHF) reference do not dissociate into two ground state nitrogen atoms, $N_2(1\Sigma_g^+) \rightarrow N(4S) + N(4S)$, and there is an unphysical maximum in the potential energy surface in the intermediate region, close to where the singlet-triplet instability occurs, at least at practical levels of CC through

CCSDT (coupled cluster singles, doubles and triples model), though CCSDTQ (coupled cluster singles, doubles, triples and quadruples model) and beyond could not be converged.⁵ Clearly this is not an ideal case for a full symmetry (D_{2h}) restricted HF reference as it would not allow for localization of electrons on the individual N atoms as would be required as the atoms separate. But perhaps the more interesting and important question is if it is possible to overcome this handicap of a bad independent particle reference at the correlated level. As a full configuration interaction (CI) or full CC calculation based on the RHF reference must get the dissociation energy and the potential energy curve (PEC) right, this suggests that the inclusion of higher excitations is important to describe the wave function and energy of the dissociating molecule at increasingly stretched geometries. Nevertheless one would not expect SR-CC to correctly describe the N_2 triple bond curve at a level less than CCSDTQPH (P-pentuples, H-hexuples) because of the usual argument that three bonds need at least hexuple excitations, and probably a bit more would be required. The indirect inclusion of the effect of these higher excitations, rather than the explicit inclusion via high-level

^{a)} Author to whom correspondence should be addressed. Electronic mail: bartlett@tp.ufl.edu

single reference methods such as CCSDTQ, CCSDTQP, and so on or through multi-reference approaches, has been an active topic of research.^{6–13}

For many years, investigators have asked the question: Can single-reference CC theory be improved by identifying cancellations among some terms present in the coupled cluster doubles (CCD) or coupled cluster singles and doubles (CCSD) approximations and higher-order cluster contributions such as those that arise from the connected quadruple cluster (T_4) and one might add by analogy, connected hextuple clusters (T_6)? If so, and if rigorous, anticipating such a cancellation would provide a computationally painless way to introduce the essential effects of T_4 . One expects that CCSDTQ¹⁴ which scales as n^{10} will do many things right that CCSD¹⁵ ($\sim n^6$), CCSDT¹⁶ ($\sim n^8$); or CCSD(T)^{17–20} ($\sim n^7$) will not. For example, whereas CCSD has to be the full CI for two electrons, CCSDTQ is that for four. So the former should be qualitatively right for most single bonds at least in the vicinity of equilibrium, while CCSDTQ would have the same property for many double bonds along with further quantifying the accuracy of CCSD and CCSDT. Another example would be bi-radicals like the benzyne isomers^{21,22} and the transition state for cyclobutadiene^{23,24} where the minimum reference space would consist of the four determinants that one can make from two nearly degenerate orbitals. One needs to include quadruple excitations to get these systems right but the “connected” part of quadruple terms (T_4) would not be naturally included in single reference theory until CCSDTQ.

Perhaps the first such suggestion of T_4 's role was that of Paldus *et al.*^{11,25} who were studying CC results for semi-empirical Hamiltonians where they knew that the exact result for a variety of different coupling strengths could be obtained by an UHF solution. Then subjecting the UHF solution to a cluster analysis relative to a RHF reference demonstrated that its inclusion of T_4 was critical to getting the right result. The direct inclusion of T_4 in the exact solution is found to be equivalent to deletion of the three (D^c , D^{ex} , and C) of the five $\frac{(T_2^2)}{2}$ diagrams shown in Figure 1. So in the absence of T_1 or when $T_1 = 0$ as for Brueckner orbitals, the approximate

coupled pair method (ACP-D45) was proposed (their diagrams 4 and 5 correspond to A and B in Fig. 1). It is equivalent to what Dykstra calls approximate CCD, or ACCD.^{26,27} This approximation was put to the test in *ab initio* theory by making applications of CCSDT to four-electron systems like H_4 ^{11,28} and observing that the effect of T_4 as measured by the difference from the full CI would have the wrong sign in the ACP-D45¹¹ = ACCD approximation. So clearly something was lacking.

Based upon their exactly soluble model problem where strong correlation meant a low or zero coupling in their semi-empirical Hamiltonian, Piecuch and Paldus¹² defined another such approximation ACP-D14 where they only retained diagrams D^c and A. This was found to be good for strong correlation effects.

By asking the question, what are the minimum number of diagrams required to get the exact answer for two-, three-, and four-electrons and all products of those units regardless of orbital choice, the n CC hierarchy⁹ was introduced. 2CC for $n = 2$, differs from ACP-D45 and ACCD only by keeping all possible T_1 terms. One aspect of 2CC was to provide a rigorous pair-like approximation that is invariant to occupied to occupied and virtual to virtual transformations unlike the conventional CEPA-1 and CEPA-2 approximations.²⁹ The critical observation that makes this possible is each diagram in CC theory individually has this orbital invariance property. So any subset of complete diagrams will manifest such invariance. 2CC retains the diagrams often termed hole-hole exclusion principle violating (EPV) diagrams, A and B in Figure 1, which are also those that configuration interaction singles and doubles (CISD) naturally includes to make that method exact for two electrons. But, of course, unlike CCSD or 2CC, CISD would not be exact for products of separated two-electron units, because CI is not size extensive.

The next step along this path was the recognition by Huntington and Nooijen⁸ that one could still accomplish the goal of a method that is exact for two-electron systems and their products as long as one factorizes the four quadratic diagrams (A, B, C, and D, $D = D^c + D^{ex}$, see Fig. 1) in the

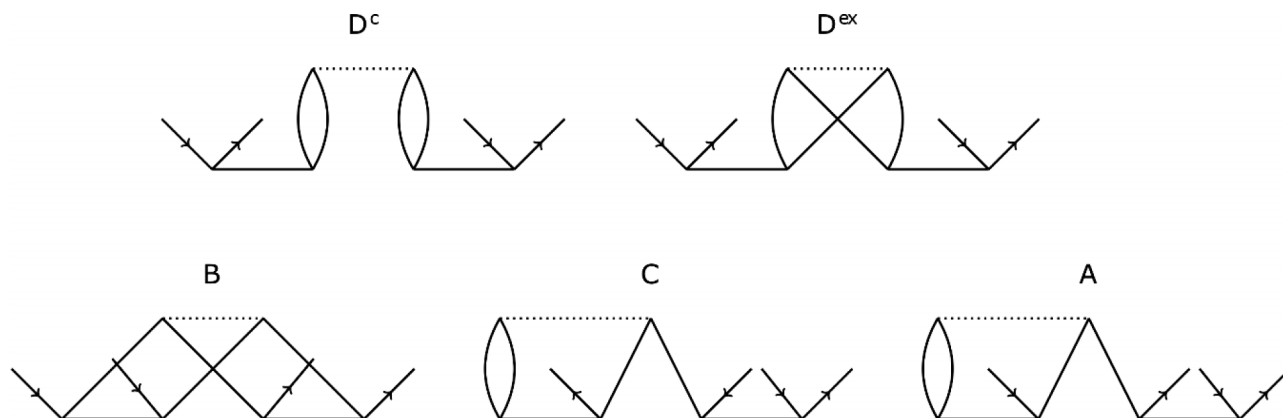


FIG. 1. Quadratic diagrams in CCD T_2 amplitude equation. The diagram D is composed of D^c and D^{ex} , its coulomb and exchange part, respectively. For DCD, the quadratic terms are $D^c + 0.5(C + A)$. Diagrams A, B, C, and D are the antisymmetrized Goldstone spin-orbital diagrams we use,¹ meaning all two-electron integrals are of the form $\langle kl||cd \rangle$. Here D is separated into D^c and D^{ex} as diagrams that are antisymmetric in T_2 amplitudes but differ by the top two-electron integral being Coulomb only, $\langle kl||cd \rangle$, in D^c with its exchange part, $\langle kl|dc \rangle$ in D^{ex} . It should be recognized that there are 11 spin-integrated, non-orthogonal Goldstone diagrams that correspond to the five quasi-antisymmetric diagrams shown for closed shells.¹

equation for the T_2 amplitude as

$$A + B + C + D = \frac{A}{2} + \alpha \left(\frac{A}{2} + B \right) + \beta(C + D).$$

This equation defines parameterized CCSD or pCCSD(α, β). For the particular choice of $\alpha = 1$ and $\beta = 0$, one regains 2CC.

Another step along this path would appear to be the distinguishable cluster (DC) approximation introduced by Kats and Manby.⁷ Suggesting that there is reason to exclude the direct exchange between the two T_2 amplitudes in Fig. 1, they separate D into a Coulomb part (D^c) and its direct exchange (D^{ex}), and exclude B entirely:

$$\begin{aligned} A + B + C + D &= A + B + C + D^c + D^{ex} \\ &= \frac{A}{2} + \gamma \left(\frac{A}{2} + B \right) + \delta \left(\frac{C}{2} + D^{ex} \right) + \frac{C}{2} + D^c. \end{aligned}$$

Choosing the values ($\gamma = 0, \delta = 0$) reduces the quadratic part of the equation to be

$$\frac{A}{2} + \frac{C}{2} + D^c.$$

This is an approximation that is exact for two electrons and has anti-symmetrized equations for the T_2 amplitudes. This choice is similar to that made in ACP-D14, except for the averaging of A and C terms and differs in its derivation owing to the orthogonal spin adaptation (OSA) approach used by Paldus.³⁰ Unlike previous choices, DC does not correspond to a fully anti-symmetric form, since the diagram D^{ex} is excluded. Nonetheless, such an approximation to the T_2 amplitudes can be computed and those amplitudes, even if there is no wave function that leads to those amplitudes, can be used in place of the usual T_1 and T_2 amplitudes to assess how well these approximations work.

Finally, a more recent effort by Scuseria *et al.*^{31,32} and by Peng *et al.*³³ elucidating connections between the random phase approximation (RPA) and CCD has also led to a related path. In particular, it is shown that the deletion of certain terms from the CCD equation sensitive to RPA instabilities helps avoid the catastrophic failures seen for CCD in strongly correlated systems.⁶ A specific method named Im-CCD (includes ladder (B) and EPV diagrams (A and C), excludes ring (D^c) and its exchange (D^{ex}) as per their

classification) seems to have an improved PEC for N_2 bond dissociation. A difference though in their approach is that modifications include deletion of linear (HT_2)_c terms as well, apart from the quadratic terms in the T_2 equation, and this method is not exact for two-electrons and their products.

Although all of the above modifications are inspired primarily to include the effects of quadruple excitations (T_4), the focus here is on N_2 , even though it might be expected to at least require the effects of connected hexuples (T_6) to obtain a qualitatively correct curve. So T_4 alone is not the answer, but the general procedure followed by the above references illustrated by T_4 is indicative of how one would hope to potentially include higher clusters to address clearly multi-reference behavior in a modified single reference framework. A numerical study of T_4 for typical four-electron problems will be published elsewhere.

II. THEORY

The Coupled Cluster theory is based on an exponential ansatz

$$|\psi_{CC}\rangle = e^{\hat{T}}|0\rangle; \hat{T} = \hat{T}_1 + \hat{T}_2 + \hat{T}_3 + \dots \quad (1)$$

The truncation of the cluster operator at a particular excitation level defines the method. The more complete the cluster operator, the better is the approximation to the exact wave function. The energy and the amplitudes are obtained by the projection

$$\begin{aligned} H_N e^{\hat{T}}|0\rangle &= \Delta E e^{\hat{T}}|0\rangle, H_N = H - \langle 0|H|0\rangle, \\ \langle 0|e^{-\hat{T}}H_N e^{\hat{T}}|0\rangle &= \Delta E, \end{aligned} \quad (2)$$

$$\begin{aligned} \langle Q|e^{-\hat{T}}H_N e^{\hat{T}}|0\rangle &= \langle Q|(H_N e^{\hat{T}})_c|0\rangle = 0, \\ Q &= \varphi_i^a, \varphi_{ij}^{ab}, \varphi_{ijk}^{abc}, \dots \end{aligned} \quad (3)$$

The CCD, $e^{T_2}|0\rangle$, method includes the complete set of double excitations and the corresponding T_2 amplitudes are obtained by solving the spin-orbital equations³⁴

$$\langle \varphi_{ij}^{ab} | (H_N(1 + T_2 + \frac{T_2^2}{2}))_c | 0 \rangle = 0, \quad \forall i, j, a, b, \quad (4)$$

i.e.,

$$\begin{aligned} t_{ij}^{ab} (\varepsilon_i + \varepsilon_j - \varepsilon_a - \varepsilon_b) &= \langle ij||ab \rangle + \frac{1}{2} \sum_{k,l} \langle ij||kl \rangle t_{kl}^{ab} + \frac{1}{2} \sum_{c,d} \langle cd||ab \rangle t_{ij}^{cd} + P(ij|ab) \sum_{c,k} \langle cj||kb \rangle t_{ik}^{ac} \\ &\quad - \frac{1}{2} P(ij) \sum_{k,l,c,d} \langle cd||kl \rangle t_{ik}^{dc} t_{lj}^{ab} + \frac{1}{4} \sum_{k,l,c,d} \langle cd||kl \rangle t_{ij}^{cd} t_{kl}^{ab} \\ &\quad - \frac{1}{2} P(ab) \sum_{k,l,c,d} \langle cd||kl \rangle t_{ik}^{ac} t_{lj}^{db} + \frac{1}{2} P(ij|ab) \sum_{k,l,c,d} \langle cd||kl \rangle t_{ik}^{ac} t_{jl}^{bd}, \quad \forall i, j, a, b. \end{aligned} \quad (5)$$

The correlation energy is obtained as

$$\Delta E = \frac{1}{4} \sum_{i,j,a,b} \langle ij||ab \rangle t_{ij}^{ab}. \quad (6)$$

If we insert the expression for t_{ij}^{ab} from (5) in (6), we obtain the total correlation energy as the sum of energy contributions from each of the constituent terms or diagrams from the T_2 equation

$$\Delta E_{CCD} = \Delta E_{MBPT(2)} + E_{L1} + E_{L2} + E_{L3} + E_{QA} + E_{QB} + E_{QC} + E_{QD}. \quad (7)$$

Here $L1$, $L2$, and $L3$ are linear terms in T_2 as in Equation (2) while quadratic terms are referred to as QC , QA , QB , and QD in correspondence with the diagrams C , A , B , and D .

$$\begin{aligned} t_{ij}^{ab} (\varepsilon_i + \varepsilon_j - \varepsilon_a - \varepsilon_b) = & \langle ij||ab \rangle + \frac{1}{2} \sum_{k,l} \langle ij||kl \rangle t_{kl}^{ab} + \frac{1}{2} \sum_{c,d} \langle cd||ab \rangle t_{ij}^{cd} + P(ij|ab) \sum_{c,k} \langle c,j||kb \rangle t_{ik}^{ac} \\ & - \frac{1}{4} P(ij) \sum_{k,l,c,d} \langle cd||kl \rangle t_{ik}^{dc} t_{lj}^{ab} - \frac{1}{4} P(ab) \sum_{k,l,c,d} \langle cd||kl \rangle t_{lk}^{ac} t_{ij}^{db} \\ & + \frac{1}{2} P(ij|ab) \sum_{k,l,c,d} \langle cd||kl \rangle t_{ik}^{ac} t_{jl}^{bd}, \quad \forall i, j, a, b. \end{aligned} \quad (8)$$

Solving these after spin integration provides the different orbital for different spin (DODS) approximation as used for UHF cases. Plugging these amplitudes into the energy expression, we can fragment the DCD energy into

$$\Delta E_{DCD} = \Delta E_{MBPT(2)} + E_{L1} + E_{L2} + E_{L3} + E_{QA} + E_{QC} + E_{QD^c}. \quad (9)$$

Note that any exclusion of terms from Equation (5) means that the wave function can no longer be expressed as $e^{T_2}|0\rangle$, and likely does not exist at all, much as there is no wave function that corresponds to the CCSD(T) method. Nonetheless, its energy and response and relaxed density matrices are still widely used.¹

The distinguishable cluster methods, DCD and DCSD are implemented in the ACES II program³⁵ as a modification of the general CCD and CCSD code. They are verified with data from the original paper by Kats and Manby.⁷ In a new development, we implement a UHF version of the program using the general spin-orbital equations in Equation (8).

Furthermore, to assess potential higher-order terms, triples corrections are added to these methods in perturbative and iterative ways as is done in CCSD(T), CCSDT-1b, and CCSDT-3, respectively. These approximations are termed DCSD(T), DCSDT-1b, and DCSDT-3. Without a rigorous prescription for how to modify or exclude diagrams for T_3 amplitudes beyond those excluded for T_2 , there is no other option. Nevertheless, we think an assessment of the triples effect is pertinent for future work.

The triple excitation amplitudes are determined through projected equations as for DCSDT-1b

$$\langle \varphi_{ijk}^{abc} | (H_N \hat{T}_2)_C | 0 \rangle = 0$$

and DCSDT-3 as

$$\langle \varphi_{ijk}^{abc} | e^{-\hat{T}_1 - \hat{T}_2} H_N e^{\hat{T}_1 + \hat{T}_2} | 0 \rangle = 0,$$

while the T_3 into T_2 and T_1 terms are the same as in the CC triples analogues.³⁴

Though this is the best that can be done to attempt some assessment of the effect of triples, response properties for

In the implementation of the Distinguishable Cluster Doubles (DCD), the T_2 amplitude equation is modified, as given in (5) for CCD, only, to eliminate the ladder diagram (B), and retain the Coulomb part of the ring diagram (D), and introduce a factor of one-half for the remaining quadratic diagrams. The equations in spin-orbital form for T_2 (DCD) are as follows:

the ground-state in DC methods are less ambiguous. They depend upon derivatives of the ground state equations which can be obtained. Hence, analytic derivatives and the relaxed and response density matrices can be immediately evaluated with formally modest, but not easily managed, changes that recognize the additional approximations in $\frac{(T_2^2)}{2}$ terms instead of those that tie to the usual infinite-order $\exp(T)$ operator. Such results will be presented in detail in a future work along with analytical gradients for any such finite method.³⁶ This, of course, is closely related to the time-dependent theory that can be used to define equation of motion based on DCSD (EOM-DCSD), which will be another component of that study.

Nonetheless, it is possible to get some idea of the results from a few EOM inspired DCSD approximations where the DCSD amplitudes are used *in lieu* of CCSD amplitudes by simple projection onto single and double excitations with modified amplitudes defining \bar{H} . This is clearly not the most rigorous answer, so we designate these approximations as E-DCD and E-DCSD, again without any modification from CC theory except for the ground state T amplitudes.

In addition, we report the “rigorous” EOM-DCD and DCSD results that replace the infinite-order \bar{H} by including appropriate modifications in the \bar{H} matrix elements so that we have a response consistent with the ground state DC approximation. See Section III G. We also use the EOM-CC and EOM-DC approximations to help tell whether a particular CC or DC solution is the lowest energy solution, the CC analogue of using RPA to assess HF stability.

All calculations on the nitrogen molecule are done using the cc-pVDZ basis set³⁷ unless mentioned otherwise, with the core orbitals frozen for the correlation calculation to be consistent with prior work. To assess any potential basis set issue, much larger TZ and QZ bases were used as well, but they show no different qualitative behavior, which is the main concern of this paper.

The stability of the HF solutions is checked with RPA calculations at various points of the PEC. This procedure helps to identify the existence of lower HF solutions and if they represent a break in spatial or spin symmetry as

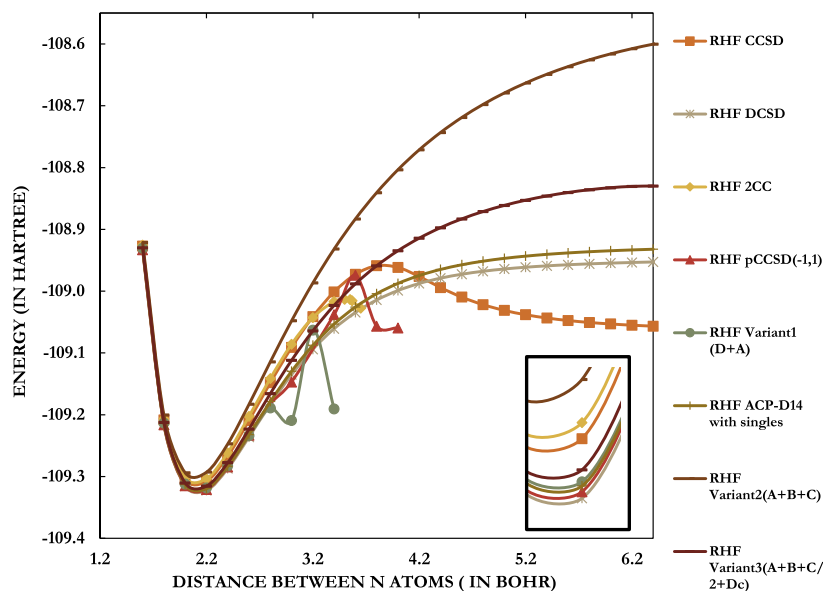


FIG. 2. Various approximate coupled cluster methods compared to CCSD for a symmetry-adapted RHF reference. Inset plot shows the relative energies for these methods near the equilibrium region.

compared to the parent solution. We identify some specific spatial symmetry broken but spin adapted RHF solutions and use them as a reference for further correlated calculations. A particular SCF solution is followed along the curve by feeding the orbitals from a previous geometry. One can run these calculations with and without symmetry. We also use EOM-CC and DC as the way to check for lower energy correlated solutions of the non-linear CC and DC equations.

In Sec. III A, the behavior of DCSD and other approximate CCSD methods for the symmetry adapted RHF reference is shown. Then we test the behavior of various triples correction to the DC approach (Sec. III B). We recognize that there would be potential room for further modification of the T_3 amplitudes for the DC approach in line with what was done for T_2 such as neglecting some higher cluster exchange terms, but lacking any prescription for which terms to delete there is no alternative. So in this first attempt, except for the changes to the T_2 amplitudes and their subsequent effect on T_1 , the same expressions are used as in CC theory.

To compare the CC and DC methods, the energy is decomposed as a sum of contributions from the linear and quadratic terms (Sec. III C). One then identifies the spatial symmetry broken RHF solutions (Sec. III D) and uses them as a reference for coupled cluster calculations under various approximations such as CCD, CCSD, CCSDT-1, CCSDT-3, and their distinguishable cluster analogs (Sec. III E). Finally, the difference among these correlation methods subject to a spin and spatially broken UHF reference (Sec. III F) is shown. The excitation energies and ionization potentials (IP's) using the EOM-DCSD approach based on a DCSD ground state (Sec. III G) are then presented.

III. RESULTS

A. Approximate coupled cluster methods: PECs based on symmetry adapted RHF reference

General coupled cluster methods (CCD, CCSD, CCSD(T), and CCSDT) are known to inaccurately describe the

N_2 dissociation process if they are based on an RHF reference that reflects the point-group symmetry of the molecule.² They have an unphysical maxima and can severely underestimate the net dissociation energy.

Interestingly, some approximations of the full CCSD method appear to overcome these qualitative deficiencies. These approximations mainly differ from each other in terms of the quadratic diagrams chosen out of the five shown in Figure 1. The corresponding PECs from these approximate CCSD methods are shown in Figure 2. Two methods that seem to have the correct features are DCSD and ACP-D14 and the common diagrams that they retain are D^c and A . By selectively introducing the D^{ex} terms as in variant1 in addition to " $D^c + A$ " as in ACP-D14, we encounter discontinuities as well as a maximum. In contrast, the 2-CC (=pCCSD (1, 0) = " $A + B$ ") method has a maximum and does not converge soon after. Another choice is pCCSD (-1, 1) which again has a rather sharp curve and a maximum. Another choice is variant3 where D^{ex} is excluded and introduce a factor of one-half to retain the exactness for 2-electron systems. The quadratic terms for this choice are " $A + B + \frac{C}{2} + D^c$ ". This would correspond to parameters ($\gamma = 1, \delta = 0$) in the DC parametrization. The curve for variant3 turns over at a more stretched geometry (not shown in Figure 2).

Motivated by lm-CCD (ladder mosaic CCD) from Scuseria and co-workers, variant2 is shown where the quadratic terms are " $A + B + C$ " and we did not modify the linear terms as is done in lm-CCD. This method gets the dissociation curve correct qualitatively but the energy at dissociation seems to be quite high. Clearly one sees that there are multiple ways of modifying the CCD/CCSD amplitude equations that can give a qualitatively correct curve.

The correct UHF-CCSDT energy for two N atoms is -108.957260 hartree ($= -54.478630 \times 2$) in this basis, which coupled with its equilibrium energy of -109.27650 hartree, gives a CCSDT dissociation energy of 200.3 kcal/mol. One can get an estimate of the dissociation energy for RHF-DCSD by subtracting the values at equilibrium with the dissociated limit which turns out to be in error by

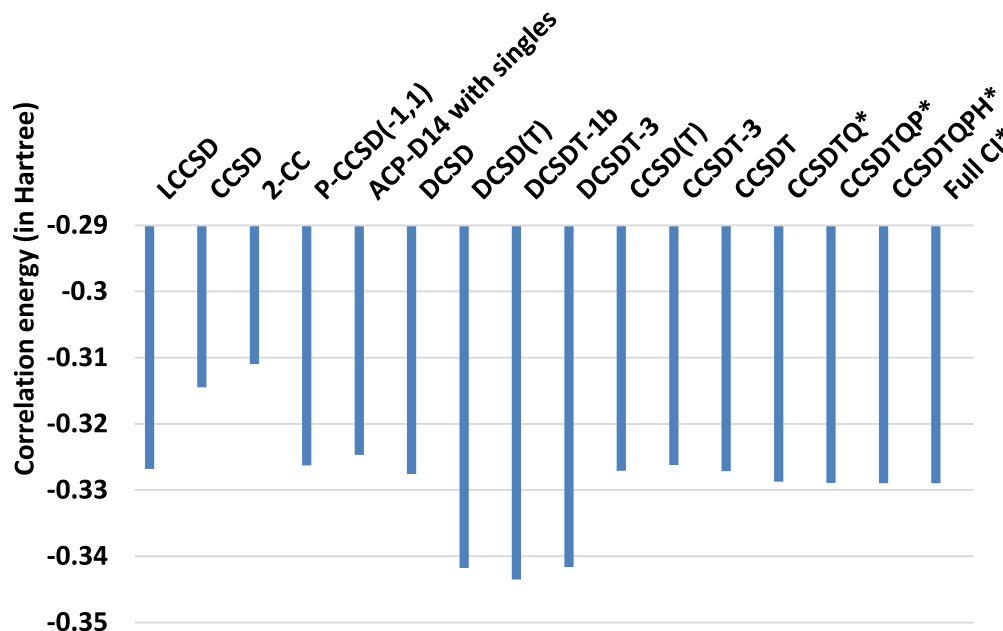


FIG. 3. Correlation energy (in hartree) for approximate CC methods compared to Full CI. The energy is relative to the RHF energy at equilibrium geometry ($r = 2.118$ bohrs). An asterisk (*) indicates data from Chan *et al.*⁵

~37 kcal/mol (−237.2 kcal/mol), while for UHF-DCSD it is 199.9 kcal/mol.

What one wants from an approximate *ab initio*, correlated method is that it gives results that can be systematically improved and converges to the exact ones (Full CI). When we compare the energies for these approximate methods with the full CI results at equilibrium, the best numerical match is with DCSD (see Figure 3), but with no variational principle or any known way to demonstrate its convergence to the right answer, this means little. In particular, any addition of the triples effect (Sec. III B) to DCSD is farther from the right answer (Table I), where we show the computed correlation energies with the cc-pVDZ basis. The correlation energies for DCSD and CCSDT compare very well even in a larger basis such as cc-pVTZ and cc-pVQZ. At equilibrium, the total correlation energy for DCSD is −0.391 095 hartree (H) and for CCSDT −0.395 337 H in the TZ basis, while it is −0.412 533 H and −0.417 892 H, respectively, in the QZ basis. The accidental agreement between the DCSD and the full CI in the small basis (DZ), and CCSDT in the large basis might imply that DCSD is an approximation that at least at equilibrium reflects the role of triples, but some rigorous cancellation would need to be proven to reach that conclusion if one believes in the “right answer for the right reason”.

B. Adding triples correction to the distinguishable cluster method: DCSD(T), DCSDT-1, and DCSDT-3

As shown in Sec. III A, the methods based on the DC approach, DCD and DCSD, using an RHF reference, have been shown to perform surprisingly well for some difficult situations which others might think require a multi-reference treatment. Interestingly, they also seem to correctly provide the qualitative nature of the PEC for the N_2 molecule, essentially overcoming the handicap of the restricted Hartree-Fock reference by changes introduced into the correlation

method. One of the goals of this work is to study why DCD and DCSD and a few other approximations seem to work well for the N_2 molecule. In Figure 4 are plotted the PECs for DCD and DCSD compared to CCSD. One can clearly see the absence of the unphysical maxima at the intermediate geometry for the distinguishable cluster based approaches as compared to the general CCSD method. But this is not always the case when we add the triples correction to it.

DCSD(T) shows a similar breakdown as CCSD(T) in the region where all finite-order perturbation methods would fail. This failure is due to the perturbative estimate (T), not the infinite order CC or DC method itself. The inclusion of triples in the DC approach is done analogously to the CCSDT-1b method and is referred to here as DCSDT-1b. The PEC for

TABLE I. Correlation Energy (in hartree) relative to the RHF at equilibrium geometry ($r = 2.118$ bohrs). ($E(\text{RHF}) = -108.949\,378$ H).

| | Correlation Energy (in hartree) |
|-----------------------|---------------------------------|
| LCCSD | −0.326 793 |
| CCSD | −0.314 493 |
| 2-CC | −0.310 946 |
| P-CCSD(−1,1) | −0.326 286 |
| ACP-D14 with singles | −0.324 672 |
| DCSD | −0.327 591 |
| DCSD(T) | −0.341 778 |
| DCSDT-1b | −0.343 487 |
| DCSDT-3 | −0.341 624 |
| CCSD(T) | −0.327 095 |
| CCSDT-3 | −0.326 206 |
| CCSDT | −0.327 122 |
| CCSDTQ ^a | −0.328 732 |
| CCSDTQP ^a | −0.328 940 |
| CCSDTQPH ^a | −0.328 959 |
| Full CI ^a | −0.328 961 |

^aSee Ref. 5.

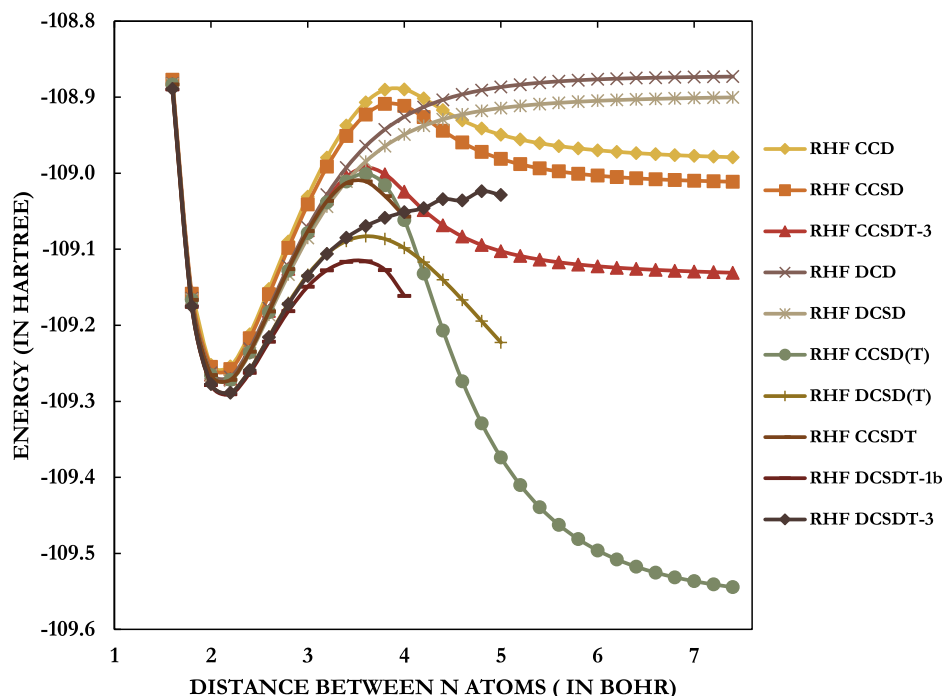


FIG. 4. DCD, DCSD, DCSD(T), DCSDT-1b, and DCSDT-3 curves compared to other CC methods for the spatial-symmetry preserved RHF reference. Notice the absence of the unphysical maxima in DCD and DCSD PES. An interesting thing to note (not depicted in this plot) is the presence of multiple solutions for the Distinguished-cluster based methods which are significantly lower in energy at the dissociation limit.

DCSDT-1b, interestingly, has a maximum in the intermediate geometry, but DCSDT-3 does not, where all T_1 and T_2 terms are included with linear T_3 , but neither can be converged at larger R . Though all wrong, the infinite-order CC approximations at least provide results at 6.4 bohrs, except for CCSDT. Various suppositions can be proposed for a more “correct” T_3 estimate but note that T-3 has quadratic T_2 contributions in T_3 while CCSDT-1a or b, does not. Should they be modified to drop the exchange contribution?

C. DCD vs CCD: Analysis of energetic contributions for each of the quadratic terms/diagrams

In this section, we analyze the individual contributions to the total correlation energy by each of the individual diagrams using expression (7) with a further breakdown of the ring diagram in terms of its Coulomb and exchange part,

$$\Delta E_{\text{CCD}} = \Delta E_{\text{MBPT}(2)} + E_{L1} + E_{L2} + E_{L3} + E_{QA} + E_{QB} + E_{QC} + E_{QD^c} + E_{QD^{\text{ex}}}.$$

Here $L1$, $L2$, and $L3$ are linear terms in T_2 as in Equation (2) while quadratic terms are referred to as QC , QA , QB , QD^c , and QD^{ex} to correspond with the diagrams C, A, B, D^c , and D^{ex} , respectively. We do this energy analysis for two situations: at equilibrium and at the dissociation limit. In the analysis below for DCD, we calculate the energy contribution from the diagrams C and A with appropriate factors included.

At equilibrium, a comparison between the CCD and DCD suggests little difference between the two methods (Table II). As the bonds are stretched, the RHF MBPT(2) energy becomes very large and negative, indicative of the quasi-degenerate nature of the underlying orbitals. A large positive correction is required to get the correct energy at the dissociation limit. This seems to be achieved by DCD to some extent by sacrificing the exchange part of the ring diagram

(D^{ex}) and the ladder diagram (B), both of which seem to be giving negative corrections to the energy (Table III). If we wanted to emulate the UHF-CC result at dissociation (see Section III F), the most expendable diagrams are B and D^{ex} , those left out in DCD. This is indicative of the effect of the natural localization engendered by UHF for this problem. Fully understanding this requires separating the effects of localization from other aspects of the UHF solution. The degree of localization of RHF solutions can be controlled to some degree by allowing spatial symmetry breaking as discussed in Sec. III D.

D. Existence of multiple restricted Hartree-Fock solutions

As the N_2 bond is stretched, the symmetry adapted RHF solution is beset by instabilities corresponding to spatial symmetry breaking (RHF and symmetry broken) or

TABLE II. Energy contributions (in hartree) near equilibrium bond distance ($r = 2.2$ bohrs). Individual quadratic contributions for CCD: $QC + QA = 0.0303$, for DCD: $2^*(QC + QA) = 0.0334$.

| | RHF-CCD | RHF-DCD |
|---------------------------------|-------------|-----------------------|
| Total energy (in hartree) | -109.253 82 | -109.267 92 |
| Total correlation energy | -0.320 71 | -0.334 81 |
| MBPT(2) energy | -0.327 45 | -0.327 45 |
| $L1$ | 0.072 44 | 0.076 39 |
| $L2$ | 0.085 29 | 0.089 81 |
| $L3$ | -0.159 60 | -0.167 08 |
| QC | 0.012 23 | 0.007 00 ^a |
| QA | 0.017 80 | 0.009 98 ^a |
| QB (ladder diagram) | -0.002 852 | ... |
| QD^c (ring diagram) | -0.020 38 | -0.023 45 |
| QD^{ex} (ring diagram) | 0.001 83 | ... |

^aEnergy contributions for diagrams C and A have a factor of one-half included for DCD method.

TABLE III. Energy contributions (in hartree) at dissociated limit ($r = 6.4$ bohrs). Comparative quadratic contributions for RHF-CCD: $QC + QA = 3.314$, for DCD: $2^*(QC + QA) = 2.537$.

| | RHF-CCD | RHF-DCD | UHF-CCD |
|--------------------------|-------------|-----------------------|-------------|
| Total energy (hartree) | -108.973 54 | -108.874 84 | -108.955 88 |
| Total correlation energy | -1.042 33 | -0.943 63 | -0.173 50 |
| MBPT(2) energy | -2.416 36 | -2.416 36 | -0.141 74 |
| $L1$ | 1.103 42 | 0.966 50 | 0.030 93 |
| $L2$ | 1.223 85 | 1.085 98 | 0.032 63 |
| $L3$ | 0.258 94 | 0.098 47 | -0.098 43 |
| QC | 1.621 97 | 0.618 49 ^a | 0.001 22 |
| QA | 1.692 20 | 0.652 24 ^a | 0.004 04 |
| QB (ladder diagram) | -0.768 75 | ... | -0.000 65 |
| QD^c (ring diagram) | -2.697 95 | -1.948 94 | -0.001 60 |
| QD^{ex} (ring diagram) | -1.056 41 | ... | 0.000 10 |

^aEnergy contributions for diagrams C and A have a factor of one-half included for the DCD method.

to both spin and spatial symmetry breaking (UHF). There exist multiple RHF solutions as one moves away from the equilibrium geometry as observed by previous studies³⁸⁻⁴⁰ and these RHF solutions are the focus of this study. Though spin-symmetry preserving, these reference solutions differ from each other in terms of the kind of spatial symmetry maintained. The spatial symmetry at the equilibrium geometry represents the abelian D_{2h} point group symmetry of the nitrogen molecule. As the bonds are stretched, the molecule tends to prefer lower symmetry giving rise to broken symmetry solutions. One categorizes the broken symmetry HF solutions by the overall symmetry of the wave function which ultimately is a reflection of the symmetry of the underlying orbitals. Here the two broken symmetry RHF solutions are of C_{2h} and C_2 symmetry,⁵³ respectively, and they are labelled by the HOMOs σ_u^- and π , of the respective reference as in Figure 5.

The UHF reference dissociates the N_2 molecule correctly leading to two nitrogen atoms in ground states of quartet spin. The spin multiplicity, $2S + 1$, for the N atom at SCF and CCSD

level, is 4.002 014 and 4.000 02, while for the N_2 molecule, it is 3.609 457 and 3.603 567, respectively, indicating an average of spin states. At dissociation, the CC energy of the N_2 molecule is double the energy of the nitrogen atom in its quartet state ($E(N_2) = 2 \times E(N(^4S))$).

The RHF wave function preserves spin symmetry, i.e., it is an eigen function of S_z and S^2 . It represents a singlet wave function throughout the potential energy surface. We investigate the differences in the three RHF solutions obtained here in terms of the spatial symmetry with consideration of the plausible localization of orbitals on the constituent fragments in the case of broken-symmetry solutions.

As has been noted before,³⁸ at the dissociation limit, one finds that the localization of each of the orbitals on either of the two atomic fragments, as in the case of the unrestricted HF wavefunction, while the full symmetry-adapted RHF solution has all orbitals delocalized over the entire supermolecule (Figure 6). Of course, a Foster-Boys or other localization could still be implemented for visualization purposes but would have no effect on the numerical results. A closer analysis of the symmetry broken HF wavefunctions is interesting as the RHF(π) solution clearly has valence MOs localized as p -orbitals on either of the two N atoms (Figure 7). All the orbital plots are generated using MacMolPlt.⁴¹

E. Coupled cluster correlation based on various RHF references

Long ago, it was noted² that coupled cluster calculations based on a D_{2h} RHF reference do not reproduce the correct nature of the potential energy curve for the breaking of the triple bond in N_2 . We see an unphysical hump in the intermediate geometry region (near the singlet-triplet instability region). This will persist to some degree for most of the coupled cluster based methods such as CCD, CCSD, CCSD(T), and CCSDT as shown in Figure 4.

In Figure 8, we have the CCSD curves for the symmetry preserved and the spatial symmetry broken RHF references

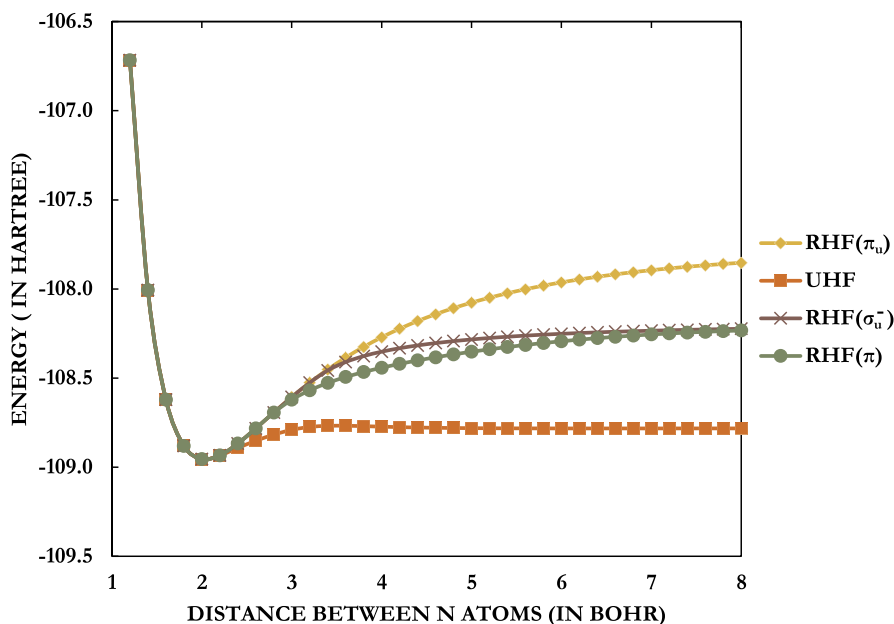


FIG. 5. Potential energy curves of multiple HF solutions, 3 spin-restricted and 1 spin-unrestricted, plotted as a function of the bond distance between N atoms. The different RHF solutions break spatial symmetry while the UHF solution represents breaking of both spin and spatial symmetry. The fully symmetry adapted RHF(D_{2h}) solution is labelled as RHF(π_u). The two broken symmetry RHF solutions are labelled by the symmetry of the HOMO and their PES is only depicted after their corresponding energies fall below the energy of the symmetry-adapted RHF solution. While the RHF(σ_u^-) has C_{2h} symmetry, the RHF(π) solution is C_2 symmetric and both of them arise at around $r = 3.0$ bohrs.

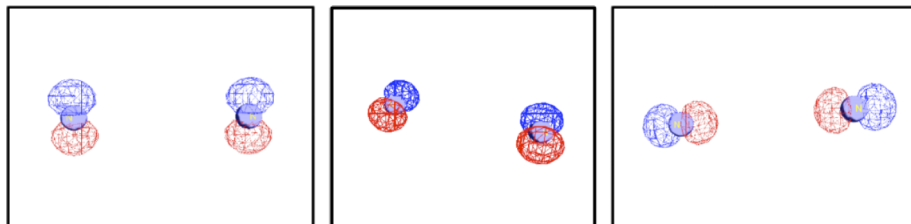


FIG. 6. HOMO, HOMO-1, and HOMO-2 Orbitals for Symmetry adapted RHF (π_u, D_{2h} symmetry) solution at dissociation ($r = 6.4$ bohrs).

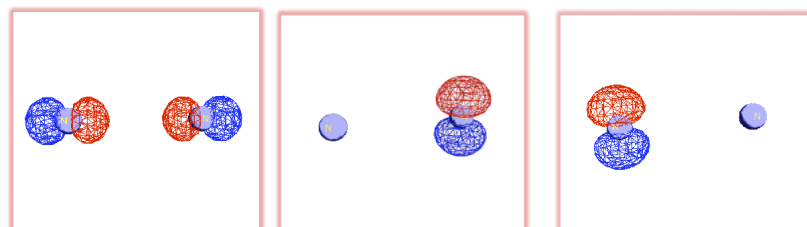


FIG. 7. HOMO, HOMO-1, and HOMO-2 orbitals for symmetry broken RHF (π, C_2 symmetry) solution at dissociation ($r = 6.4$ bohrs) showing localization of electrons on the respective atoms.

studied. Curiously, one sees that CCSD based on a symmetry broken reference shows a qualitatively correct curve with the local maxima absent.

The curves generated with the CCD/CCSD/CCSDT-3 method based on some spatial symmetry broken RHF references do not have the maxima in the bond-dissociation curve (Figure 9). It is indicative of the partial localization of the electrons already introduced at the reference level due to the breaking of spatial symmetry. The most complete curve here is CCSD. Though it is generally true that breaking of spatial symmetry fixes the problem with the reference, some of the CC and DC based PEC using broken symmetry RHF references retain the maxima as well as a discontinuity including DCD (Fig. 10).

We note here that the existence of multiple coupled-cluster solutions, increasingly so at stretched bond geometries, plagues our study. The occurrence of these multiple solutions might be symptomatic of a strong correlation scenario in general as has been found by a recent study.⁴² Initially, we tried to overcome this problem by using a guess for

T -amplitude coefficients from a previous geometry point. At times, the energetic reordering of constituent orbitals at multiple geometry points as is seen in broken symmetry RHF(π) solution presents an artefactual problem leading to convergence to the wrong solution. This, of course, is fixed by reordering the T -amplitudes to reflect the change in the ordering of the constituent orbitals. But still we could not resolve all discontinuities and singularities on the CC potential energy surfaces. Thus, we used excitation calculations using the EOM-CC route as a check for the existence of lower energy CC solutions that would correspond to negative excitation energies. In this way, EOM-CC is essentially the CC analog of using RPA to check for HF stability. Using amplitudes from the observed lower energy eigenvector R_k revealed by EOM-CC as a starting guess for a ground state CC solution sometimes resolved the convergence issue.

For the RHF (π, C_2 symmetry) solution, the distinguishable cluster based methods, DCD and DCSD, have discontinuities in the curve. We speculate that there might

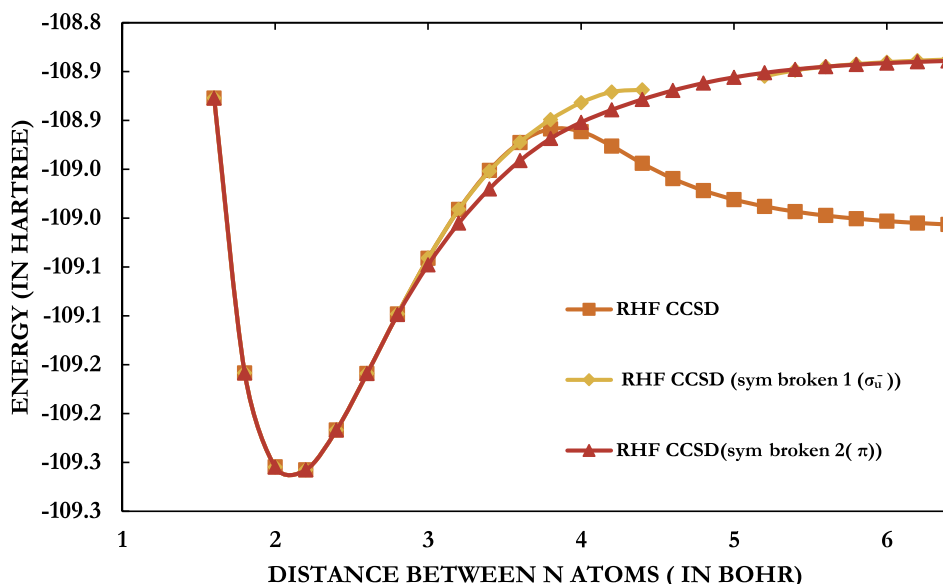


FIG. 8. CCSD curves based on different RHF references. Note the seeming discontinuity in the singlet-triplet region for one of the symmetry broken solutions, the well documented unphysical hump in the completely symmetry preserved RHF solution. The curves for the two symmetry broken solutions almost overlap at distances far away from the equilibrium geometry. Note also a discontinuity for a small region (4.6–5.0 bohrs) for one of the symmetry-broken solution (C_{2h} symmetry). It seems one can extrapolate in this region and regain the curve again at 5.0 bohrs.

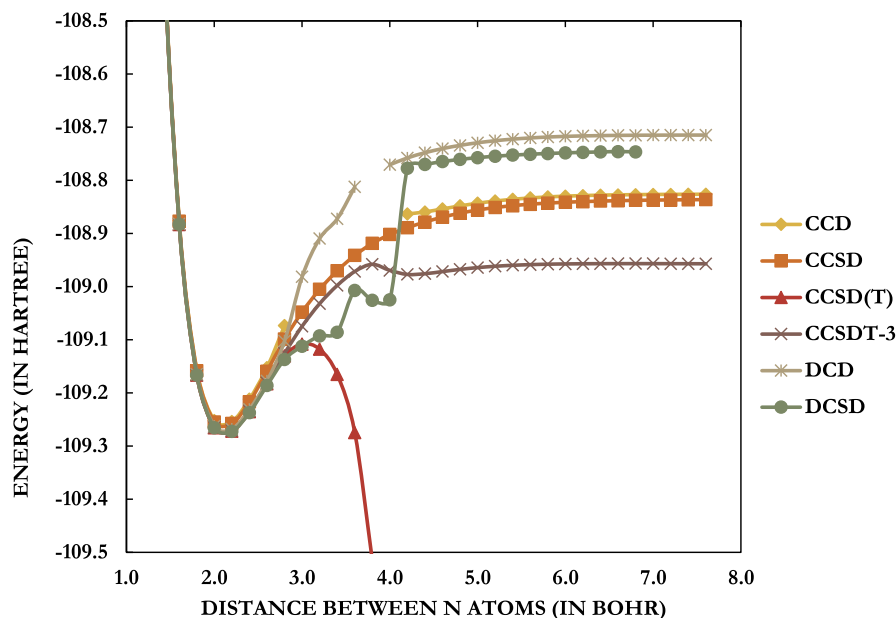


FIG. 9. PES for different CC methods, CCD and DCSD, using symmetry broken RHF (π , C_2 symmetry) solution.

exist a lower energy solution for these methods but we could not find it by varying our starting guesses of T -amplitudes. We also played with E-DCSD and EOM-DCSD calculations at various points and did get lower energy solutions but as estimated by their total energy, they did not necessarily appear to be physically meaningful ones.

Discontinuities are also seen for coupled cluster calculations based on the other symmetry broken solution studied here (Figure 10). To extend the PEC for DCSD which sees a switch to a distinct higher energy solution for $r > 4.2$ bohrs, we use E-DCSD to obtain the total energy for the correct CC state.

A word about such discontinuities. Once one is encountered, the behavior as shown on the plotted curve is arbitrary, as it is subject to the particular algorithm used in the calculation and cannot be reproduced. Nonetheless,

they are shown as they occur in our calculation. When we find different solutions via different starting guesses or by exploring the EOM-CC solutions, we can complete some of these curves with confidence, but the parts in between, and the extensive oscillations seen, have no meaning beyond pointing out the discontinuity.

To answer the question about the possible use of these symmetry broken solutions as a reference for correlated calculations, we compare the total correlation energy and total energies recovered for these references as compared to that for the symmetry preserved RHF solution (see Table IV). On comparing the energy contributions for each of the linear and quadratic diagrams for different RHF references, the magnitude of the terms seem to be smaller in size for the symmetry-broken references as compared to the fully symmetric RHF reference.

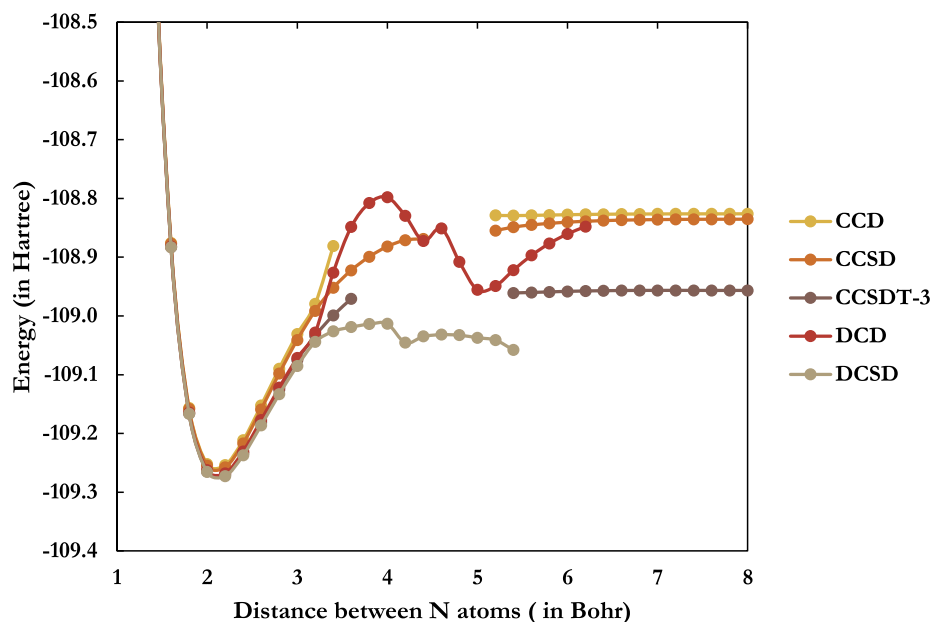


FIG. 10. Another broken symmetry reference (σ_u^- , C_{2h} symmetry) used for correlation calculations. We see maxima at around $r = 4$ bohrs for DCD and a discontinuity in the intermediate region ($r = 4-5$ bohrs) for CCD, CCSD, and CCSDT-3 while a sudden jump to a higher energy solution is observed for DCSD.

TABLE IV. Energy contributions for Coupled Cluster Doubles (CCD) based on different references (in hartree) at dissociated limit ($r = 6.4$ bohrs).

| | RHF-CCD (symmetry adapted reference, HOMO- π_u) | RHF-CCD (symmetry broken reference, HOMO- π , C_2) | RHF-CCD (symmetry broken reference, HOMO- σ_u^- , C_{2h}) | UHF-CCD |
|--------------------------|--|---|---|-------------|
| Total energy (H) | -108.973 54 | -108.827 93 | -108.826 83 | -108.955 88 |
| Total correlation energy | -1.042 33 | -0.552 23 | -0.583 67 | -0.173 50 |
| MBPT(2) energy | -2.416 36 | -0.360 57 | -0.423 51 | -0.141 73 |
| L_1 | 1.103 42 | 0.395 74 | 0.480 09 | 0.030 93 |
| L_2 | 1.223 85 | 0.403 60 | 0.488 27 | 0.032 63 |
| L_3 | 0.258 94 | -1.104 12 | -1.317 59 | -0.098 43 |
| QC | 1.621 97 | 0.217 93 | 0.350 07 | 0.001 22 |
| QA | 1.692 20 | 0.256 60 | 0.396 40 | 0.004 04 |
| QB (ladder diagram) | -0.768 75 | -0.104 15 | -0.167 35 | -0.000 65 |
| QD^c (ring diagram) | -2.697 95 | -0.111 65 | -0.177 37 | -0.001 60 |
| QD^{ex} (ring diagram) | -1.056 41 | -0.145 61 | -0.212 72 | 0.000 10 |

F. Coupled cluster calculations based on unrestricted Hartree-Fock reference: How do DC based methods perform?

A UHF reference allows for breaking of both spatial and spin symmetries. As for restricted reference, multiple spatial-symmetry broken solutions exist for unrestricted HF references as well.⁴³ In particular, the loss of inversion symmetry⁴⁴ is the key factor to get the description of dissociated N atoms right. The correlation calculations, those based on coupled cluster theory using a UHF reference (C_2 symmetry) seem to capture most of the essential features of the correct potential energy surface for bond-breaking in the nitrogen molecule: an approximately correct dissociation energy of 200.3 kcal/mol (CCSDT, cc-pVDZ basis) and an absence of unphysical local maxima before complete bond dissociation. There is still the well-known curvature change in the spin recoupling region as is seen on the UHF PEC in Figure 5. Here we have the PES generated with various levels of approximations for the CC method (see Figure 11). We generalize the distinguished cluster methods to be based on the unrestricted HF reference. The results suggest that there is a very small difference between the performance of the general coupled cluster methods and the distinguishable cluster methods based on a UHF reference. So natural

localization at the separated limit removes the distinction which would be consistent with the idea of no exchange between T_2 amplitudes.

G. Vertical excitation energies and IPs through EOM-DCD and EOM-DCSD

As derivatives of approximate CC equations (collectively called pCC for parameterized CC methods) and their energies define molecular properties, whether static or dynamic, the fundamental quantity required is the associated functional, composed of an energy expression subject to a constraint that the defining equations are satisfied. For an approximate doubles ground state,

$$\Delta\mathcal{E} = \langle 0 | (H_N \left(1 + T'_2 + \frac{(T'_2)^2}{2} \right))_C | 0 \rangle + \sum_q \lambda_q \langle \phi_q | (H_N \left(1 + T_2 + \frac{(T_2)^2}{2} \right))_C | 0 \rangle \quad (10)$$

$$= \langle 0 | (1 + \Lambda) (H_N \left(1 + T'_2 + \frac{(T'_2)^2}{2} \right))_C | 0 \rangle, \quad (11)$$

where the second form is the approximate pCC functional for the method. Variation with respect to λ obviously gives the

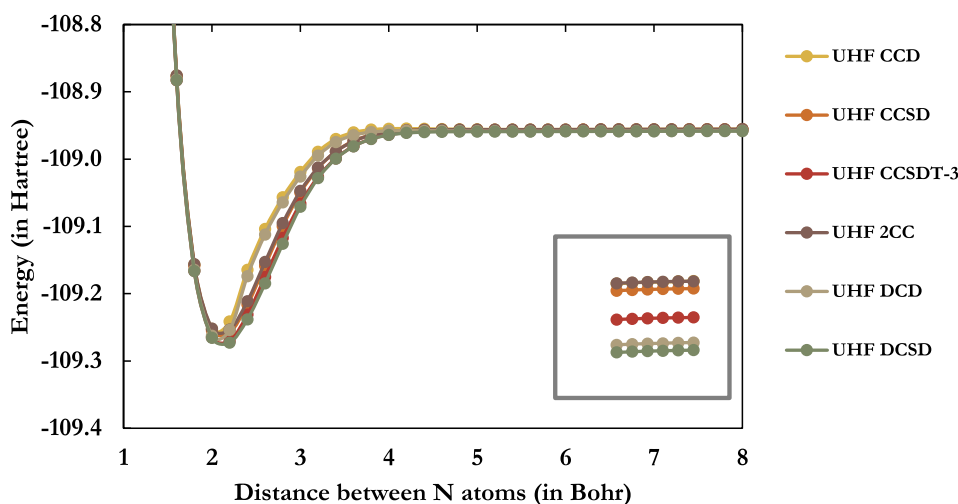


FIG. 11. PECs generated by different CC method based on UHF reference. Inset plot shows the ordering of the energies for each method at dissociation limit.

amplitude equations for pCC , while variation with respect to T_2' gives

$$\delta\Delta\mathcal{E} = \langle 0 | \delta(H_N \left(1 + T_2' + \frac{(T_2')^2}{2}\right))_C | 0 \rangle + \sum_q \lambda_q \langle \phi_q | \delta(H_N \left(1 + T_2' + \frac{(T_2')^2}{2}\right))_C | 0 \rangle. \quad (12)$$

We use the expression below to define an effective Hamiltonian (H_{eff})

$$\delta(H_N \left(1 + T_2' + \frac{(T_2')^2}{2}\right))_C = [H_{eff}, \delta T_2']. \quad (13)$$

Then

$$\langle 0 | [H_{eff}, \delta T_2'] | 0 \rangle + \sum_q \lambda_q \langle \phi_q | [H_{eff}, \delta T_2'] | 0 \rangle = 0, \quad (14)$$

$$\langle 0 | H_{eff} \delta T_2' | 0 \rangle - \langle 0 | \delta T_2' H_{eff} | 0 \rangle + \sum_q \lambda_q \langle \phi_q | H_{eff} \delta T_2' | 0 \rangle - \sum_q \lambda_q \langle \phi_q | \delta T_2' H_{eff} | 0 \rangle = 0.$$

Defining pCC energy as $H_{eff} | 0 \rangle = E_{pCC} | 0 \rangle$,

$$\begin{aligned} \langle 0 | H_{eff} \delta T_2' | 0 \rangle + \sum_q \lambda_q \langle \phi_q | H_{eff} \delta T_2' | 0 \rangle - \sum_q \lambda_q E_{pCC} \langle \phi_q | \delta T_2' | 0 \rangle &= 0, \\ \langle 0 | H_{eff} \delta T_2' + \sum_q \lambda_q \langle \phi_q | H_{eff} \delta T_2' - \sum_q \lambda_q E_{pCC} \langle \phi_q | \delta T_2' &= 0, \\ \langle 0 | H_{eff} \delta T_2' + \sum_q \lambda_q \langle \phi_q | H_{eff} \delta T_2' - \sum_q \lambda_q E_{pCC} \langle \phi_q | \delta T_2' &= 0, \\ \langle 0 | H_{eff} + \sum_q \lambda_q \langle \phi_q | (H_{eff} - E_{pCC}) &= 0. \end{aligned} \quad (15)$$

This leads us to the Λ equations

$$PH_{eff} + \Lambda_{pCC} Q(H_{eff} - E_{pCC}) = 0; \quad P + Q = 1, \quad P = | 0 \rangle.$$

Since the origin of Λ in the general CC case^{1,24} shows that $\Lambda = P\bar{H}(E_{CC} - \bar{H})^{-1}Q$, and further that $\frac{\partial T}{\partial \lambda}|_{\lambda=0} = Q(E_{CC} - \bar{H})^{-1}Q \frac{\partial H}{\partial \lambda}|_{\lambda=0}$ in perturbation theory, the critical quantity in EOM-CC is the resolvent operator, $Q(E_{CC} - \bar{H})^{-1}Q$. When writing down the dynamic polarizability,⁴⁵ the important change is that the resolvent then reads, $Q(E_{CC} - \bar{H} \pm \omega)^{-1}Q$, and the eigenvalues of $(E_{CC} - \bar{H})$, thus, have to correspond to excitation energies, the poles of the polarization propagator. So for any parameterized CC method, DCD, or the others we discussed, the critical change is in the determination of the \bar{H} equivalent for pCC or H_{eff} as derived above, and that ties to Λ_{pCC} . The determination of the static polarizability verifies that Λ_{pCC} is correct, which can be checked by finite-field calculations with pCC . The explicit expressions for H_{eff} will be discussed in more detail in a paper to be published³⁶ where both analytical gradients and $EOM-pCC$ results will be presented.

If one tried to obtain excited states and excitation energies simply by taking the T_1' and T_2' amplitudes obtained for the DCD and DCSD reference state to construct the usual \bar{H} matrix (as in EOM-CCSD), one gets the E-DCD and E-DCSD approximations, to distinguish them from the EOM-DCD and DCSD, which properly accommodate the lack of a wavefunction and the truncated form of the pCC approximations above. The vertical excitation energies for

the N_2 and CO molecules using a cc-pVQZ basis set⁴⁶ are reported in Table V.

In every case, the EOM approximations are better than those given by the E approximation, as consistency would dictate. There does not seem to be much difference in the ground state description, since even EOM-CCD and EOM-CCSD tend to be quite close (both have singles, R_1 , and doubles, R_2 , expansions in the excited states) reflecting the comparative insensitivity that the EOM treatment of excited states shows toward the description of the ground state. The major distinction between EOM-CCSDT and the lower approximations is the expanded space of all triple excitations, R_3 , being added to the \bar{H} matrix, not the triples in the ground state. Clearly, E-DCD and E-DCSD are 0.1-0.3 eV farther away from the excitation energies predicted by EOM-CCD and EOM-CCSD for the states studied here (Table V). But we see a dramatic improvement for EOM-DCD and EOM-DCSD, though they vary from 0.15 to -0.15 eV from their EOM-CCD and EOM-CCSD counterparts, respectively.

Similarly, one can calculate the ionization potentials through an IP-EOM calculation in a cc-pVQZ basis and find that the ordering of orbitals for DCSD is as expected from IP-EOM CCSD and IP-EOM-CCSDT calculations. The IP estimates through E-DCSD differ by 0.1-0.15 eV from those for IP-EOM-CCSD while those for IP-EOM-DCSD are comparable (Table VI).

A more detailed study on excitation energies, the spectrum of other IP, EA, DIP, and DEA results, and related properties

TABLE V. Vertical excitation energies (in eV) for the N₂ and CO molecules from EOM-DCD and DCSD compared to EOM-CC (equilibrium distance for N₂⁴⁷ = 2.065 659 4 bohrs, Equilibrium distance for CO⁴⁷ = 2.124 619 08 bohrs).

| | State | E-DCD | EOM-DCD | EOM-CCD | E-DCSD | EOM-DCSD | EOM-CCSD | EOM-CCSDT ⁴⁷ | Expt. ^a |
|----------------|--|-------|---------|---------|--------|----------|----------|-------------------------|--------------------|
| N ₂ | ¹ Π _g | 9.77 | 9.47 | 9.58 | 9.72 | 9.43 | 9.54 | 9.36 | 9.31 |
| | ¹ Σ _u ⁻ | 10.37 | 10.27 | 10.14 | 10.40 | 10.30 | 10.16 | 9.93 | 9.92 |
| | ¹ Δ _u | 10.80 | 10.69 | 10.57 | 10.84 | 10.73 | 10.60 | 10.34 | 10.27 |
| CO | ¹ Π | 8.90 | 8.70 | 8.77 | 8.84 | 8.63 | 8.71 | 8.56 | 8.51 |
| | ¹ Σ ⁻ | 10.21 | 9.99 | 10.04 | 10.39 | 10.16 | 10.20 | 10.00 | 9.88 |
| | ¹ Δ | 10.33 | 10.09 | 10.17 | 10.53 | 10.28 | 10.34 | 10.14 | 10.23 |

^aFor experimental values.⁴⁸

TABLE VI. Ionization potential (in eV) for N₂ and CO molecules for IP-EOM-DCSD and IP-EOM-CC.

| | Nominal state | IP-E-DCSD | IP-EOM-DCSD | IP-EOM-CCSD | IP-EOM-CCSDT ⁴⁹ | Expt. |
|----------------|-----------------|-----------|-------------|-------------|----------------------------|-------|
| N ₂ | 3σ _g | 15.76 | 15.47 | 15.68 | 15.55 | 15.60 |
| | 1π _u | 17.42 | 17.31 | 17.28 | 16.99 | 16.98 |
| | 2σ _u | 19.04 | 18.58 | 18.94 | 18.77 | 18.78 |
| CO | 5σ | 14.27 | 14.08 | 14.22 | 13.98 | 14.01 |
| | 1π | 17.26 | 17.03 | 17.13 | 17.05 | 16.91 |
| | 4σ | 19.97 | 19.56 | 19.86 | 19.64 | 19.72 |

from the relaxed and response density matrices using DCSD and other approximate *pCC* methods will be published elsewhere.³⁶

IV. CONCLUSIONS

The inclusion of the effects of higher excitations is very important in obtaining correct results for quasi-degenerate situations. The problem of the simultaneous breaking of multiple bonds is one such situation where it has been found that one can systematically correct fallacies inherent in a simple approximation such as CCD by inclusion of higher excitations. The failure of lower-level single reference based correlation methods to describe breaking of the triple bond in the nitrogen molecule is an illustrative example. The question to ask then, can a correlation method, which uses a physically incorrect (symmetry preserved RHF) reference throughout the potential energy curve, correct the fallacies connected to the reference and produce a plausible PEC? This is the intrigue offered by the fact that the distinguishable cluster methods and some other *pCC* approximations seem to be able to achieve the above by suitable removal of terms from the amplitude equation or “addition by subtraction.” This is also true of ACP-D14, as the major villain is the exchange term that arises from the $\frac{(T_2^2)}{2}$ ring diagram. Results based on the energy analysis of the individual diagrams show that leaving out specific terms with large negative energy corrections at stretched geometries is the reason for the relatively good performance of this approach, which is not quite as obvious to the cynic who would say leaving out any positive energy terms will inevitably lower the total energy and give a better, if unjustified approximation. Linearized CCSD does much the same thing when all quadratic terms

are removed, but does suffer from singularities as the solution to a linear equation when not handled carefully.⁵⁰ UHF based CC and DC methods naturally de-emphasize the excluded terms due to the ability of the UHF MOs to localize at large separation, and that aids in producing the best obtained results.

We speculate that one justification for removal of the terms left out in the distinguishable cluster approach is their probable cancellation by terms involving higher excitation clusters. This is to be confirmed by more quantitative and theoretical reasoning and will be the subject of a future work.

Kats *et al.*^{7,51} argued that the distinguishable cluster approach seeks to remove what they believe to be unphysical exchange between two dissociating fragments which would be the case if the electrons were to be localized on the individual fragments, but, of course, does not apply when there is no spatial distinction. This leads us to speculate about the possible use of symmetry broken RHF references present which themselves allow for partial localization of electrons on the individual fragments depending on the kind of spatial symmetry preserved. Doing so helped CC methods work as well or better than DC methods. We also think some of these spatial symmetry broken reference solutions might be of use as references for correlation calculations especially in bond-breaking situations. From another viewpoint, can suitable localization in separated units facilitate a better description of that limit without symmetry breaking?

We probe the multiple symmetry broken RHF solutions that arise as we stretch the bond in the nitrogen molecule and use them as a reference for coupled cluster calculations. Familiar issues of non-convergence arise while the existence of multiple CC energy solutions for the same HF reference complicates the analysis. Detailed studies need to be done to arrive at a possible prescription for the “right” CC solution

based on the symmetry of the final CC wave function based on the T -amplitude coefficients and if they obey the degeneracies seen in the underlying orbitals in the reference. We find that DC methods perform worse than CC ones for these spatial symmetry broken references.

Systematic generalization of DC or other pCC methods to include higher excitations requires attention. Can the argument about the need to eliminate unphysical exchange between dissociating fragments by excluding a particular set of quadratic diagrams (T_2^2) be extended to higher excitation clusters (T_3^2) or to cubic terms (T_2^3)? In particular, the factorized quadruples⁵² (Q_f) approximation ($\sim n^7$) to a full quadruples via CCSDTQ, also arises from consideration of $T_2^\dagger W \frac{T_2}{2}$, so should the last part of the expression be split into a Coulomb and exchange part? And if so, why? When we add corrections due to triple excitations to the DC methods in a way similar to the CC methods, the results are no longer a good match with the expected full CI result, but greatly overshoot. The true believer would say this is due to connected triples already being included into the result via the DCSD approximations, but others would say this is due to the simple expedient of leaving out some positive terms. DCSD appears to be good for the standard RHF reference, but not for spatial symmetry broken references.

We report a UHF based implementation of the distinguished cluster methods, DCD and DCSD. We conclude that all the CC (DCD and DCSD included) correlation methods perform equally well for the UHF reference when we allow the breaking of both spatial and spin symmetry. This means that the usefulness of the DC approach would seem to be limited to making a fully symmetry adapted RHF reference work without appealing to symmetry broken references, as is seen here for the case of N_2 . Whether that effect can be explained by the indirect inclusion of higher cluster amplitudes like T_4 , T_5 , T_6 , and higher, is a task to be addressed. The DODS implementation also opens the door to assessing such pCC methods for open-shell systems.

Finally, the initial EOM-DCSD results for ionization potentials and excitation energies are about the same as those from EOM-CCSD. However, if the latter diverges subject to incorrectly separating RHF references while the former does not, then the EOM-DCSD would have an advantage in the separated atom limit when many PECs might be required as a function of R .

ACKNOWLEDGMENTS

The work has been supported by the AFOSR under Grant No. FA9550-14-1-0281. We thank Dr. Daniel Kats for providing the details of his calculations which were used to verify our implementation of DCD and DCSD. We are grateful to Professor Marcel Nooijen for providing us access to the pCCSD code and insightful comments on the manuscript. We would also like to thank Professor Josef Paldus and Dr. Dmitry Lyakh for helpful discussions.

¹R. J. Bartlett and M. Musiał, *Rev. Mod. Phys.* **79**, 291 (2007).

²W. D. Laidig, P. Saxe, and R. J. Bartlett, *J. Chem. Phys.* **86**, 887 (1987).

³P. Piecuch, S. A. Kucharski, and K. Kowalski, *Chem. Phys. Lett.* **344**, 176 (2001).

⁴J. W. Krogh and J. Olsen, *Chem. Phys. Lett.* **344**, 578 (2001).

⁵G. K.-L. Chan, M. Kállay, and J. Gauss, *J. Chem. Phys.* **121**, 6110 (2004).

⁶T. W. Bulik, T. M. Henderson, and G. E. Scuseria, *J. Chem. Theory Comput.* **11**, 3171 (2015).

⁷D. Kats and F. R. Manby, *J. Chem. Phys.* **139**, 021102 (2013).

⁸L. M. J. Huntington and M. Nooijen, *J. Chem. Phys.* **133**, 184109 (2010).

⁹R. J. Bartlett and M. Musiał, *J. Chem. Phys.* **125**, 204105 (2006).

¹⁰D. W. Small and M. Head-Gordon, *J. Chem. Phys.* **137**, 114103 (2012).

¹¹K. Jankowski and J. Paldus, *Int. J. Quantum Chem.* **18**, 1243 (1980).

¹²P. Piecuch and J. Paldus, *Int. J. Quantum Chem.* **40**, 9 (1991).

¹³T. Van Voorhis and M. Head-Gordon, *Chem. Phys. Lett.* **330**, 585 (2000).

¹⁴S. A. Kucharski and R. J. Bartlett, *J. Chem. Phys.* **97**, 4282 (1992).

¹⁵G. D. Purvis and R. J. Bartlett, *J. Chem. Phys.* **76**, 1910 (1982).

¹⁶J. Noga and R. J. Bartlett, *J. Chem. Phys.* **86**, 7041 (1987).

¹⁷M. Urban, J. Noga, S. J. Cole, and R. J. Bartlett, *J. Chem. Phys.* **83**, 4041 (1985).

¹⁸K. Raghavachari, G. W. Trucks, J. A. Pople, and M. Head-Gordon, *Chem. Phys. Lett.* **157**, 479 (1989).

¹⁹R. J. Bartlett, J. D. Watts, S. A. Kucharski, and J. Noga, *Chem. Phys. Lett.* **165**, 513 (1990).

²⁰J. D. Watts, J. Gauss, and R. J. Bartlett, *J. Chem. Phys.* **98**, 8718 (1993).

²¹C. J. Cramer, J. J. Nash, and R. R. Squires, *Chem. Phys. Lett.* **277**, 311 (1997).

²²X. Li and J. Paldus, *J. Chem. Phys.* **129**, 174101 (2008).

²³A. Balková and R. J. Bartlett, *J. Chem. Phys.* **101**, 8972 (1994).

²⁴M. Musiał, A. Perera, and R. J. Bartlett, *J. Chem. Phys.* **134**, 114108 (2011).

²⁵J. Paldus, J. Čížek, and M. Takahashi, *Phys. Rev. A* **30**, 2193 (1984).

²⁶R. A. Chiles and C. E. Dykstra, *J. Chem. Phys.* **74**, 4544 (1981).

²⁷R. A. Chiles and C. E. Dykstra, *Chem. Phys. Lett.* **80**, 69 (1981).

²⁸S. Kucharski, A. Balková, and R. J. Bartlett, *Theor. Chim. Acta* **80**, 321 (1991).

²⁹R. Ahlrichs, *Comput. Phys. Commun.* **17**, 31 (1979).

³⁰J. Paldus, *J. Chem. Phys.* **67**, 303 (1977).

³¹G. E. Scuseria, T. M. Henderson, and D. C. Sorensen, *J. Chem. Phys.* **129**, 231101 (2008).

³²G. E. Scuseria, T. M. Henderson, and I. W. Bulik, *J. Chem. Phys.* **139**, 104113 (2013).

³³D. Peng, S. N. Steinmann, H. Van Aggelen, and W. Yang, *J. Chem. Phys.* **139**, 104112 (2013).

³⁴I. Shavitt and R. J. Bartlett, *Many-Body Methods in Chemistry and Physics: MBPT and Coupled-Cluster Theory* (Cambridge University Press, 2009).

³⁵J. F. Stanton, J. Gauss, S. A. Perera, A. Yau, J. D. Watts, M. Nooijen, N. Oliphant, P. G. Szalay, W. J. Lauderdale, S. R. Gwaltney, S. Beck, A. Balková, D. E. Bernholdt, K. K. Baec, P. Rozyczko, H. Sekino, C. Huber, J. Pittner, and R. J. Bartlett, ACESII is a product of the quantum theory project, University of Florida, 2005. Integral packages included are VMOL (J. Almólf and P. R. Taylor), VPROPS (P. R. Taylor), and ABACUS (T. Helgaker, H. J. A. Jensen, P. Jørgensen, J. Olsen, and P. R. Taylor).

³⁶A. Perera, V. Rishi, and R. J. Bartlett, "Analytical gradients and equation of motion techniques for excited states for simplified coupled cluster methods" (unpublished).

³⁷T. H. Dunning, *J. Chem. Phys.* **90**, 1007 (1989).

³⁸X. Li and J. Paldus, *J. Chem. Phys.* **130**, 084110 (2009).

³⁹A. J. W. Thom and M. Head-Gordon, *Phys. Rev. Lett.* **101**, 193001 (2008).

⁴⁰S. Veeraraghavan and D. A. Mazziotti, *Phys. Rev. A* **89**, 010502 (2014).

⁴¹B. M. Bode and M. S. Gordon, *J. Mol. Graphics Model.* **16**, 133 (1998).

⁴²R. Podaszwa and L. Z. Stolarczyk, *Chem. Phys. Lett.* **366**, 426 (2002).

⁴³A. Igawa and H. Fukutome, *Prog. Theor. Phys.* **64**, 491 (1980).

⁴⁴J. D. Watts and R. J. Bartlett, *J. Chem. Phys.* **95**, 6652 (1991).

⁴⁵P. B. Rozyczko, S. A. Perera, M. Nooijen, and R. J. Bartlett, *J. Chem. Phys.* **107**, 6736 (1997).

⁴⁶D. E. Woon and T. H. Dunning, *J. Chem. Phys.* **103**, 4572 (1995).

⁴⁷M. Musiał and S. A. Kucharski, *Struct. Chem.* **15**, 421 (2004).

⁴⁸J. Oddershede, N. E. Grüner, and G. H. F. Diercksen, *Chem. Phys.* **97**, 303 (1985).

⁴⁹M. Musiał, S. A. Kucharski, and R. J. Bartlett, *J. Chem. Phys.* **118**, 1128 (2003).

⁵⁰A. G. Taube and R. J. Bartlett, *J. Chem. Phys.* **130**, 144112 (2009).

⁵¹D. Kats, D. Kreplin, H.-J. Werner, and F. R. Manby, *J. Chem. Phys.* **142**, 064111 (2015).

⁵²S. A. Kucharski and R. J. Bartlett, *J. Chem. Phys.* **108**, 9221 (1998).

⁵³This broken symmetry solution has been referred to as a C_{2v} symmetry solution in the literature.^{38,40}